A Novel Mercury-Sensitive Fluorescent Nano-chemosensor using new Functionalized Magnetic core-shell Fe$_3$O$_4$@SiO$_2$ Nanoparticles

Hosseini, M.[1], Memari, Z.[2], Ganjali, M.R.[2*], Khoobi, M.[3], Faridbod, F.[2], Shafiee, A.[3,4], Norouzi, P.[2], Shamsipur, M.[5] and Hajinezhad, A.[6]

[1] Department of life science engineering, Faculty of New Sciences & Technologies, University of Tehran, Tehran, Iran

[2] Center of Excellence in Electrochemistry, Faculty of Chemistry, University of Tehran, Tehran, Iran

[3] Pharmaceutical Sciences Research Center, Tehran University of Medical Sciences, Tehran 14176, Iran

[4] Department of Medicinal Chemistry, Faculty of Pharmacy and Pharmaceutical Sciences Research Center, Tehran University of Medical Sciences, Tehran 14176, Iran

[5] Department of Chemistry, Razi University, Kermanshah, Iran

[6] Faculty of New Sciences & Technologies, University of Tehran, Tehran, Iran

ABSTRACT: In this work, a novel Hg^{2+} sensitive fluorescent chemosensor is constructed. The proposed nano-chemosensor was prepared through the preparation of 3-(benzo[*d*]thiazol-2-yl)-7-hydroxy-2*H*-chromen-2-one functionalized silica nanoparticles which has high magnetization properties (BTC-Fe$_3$O$_4$@SiO$_2$). The ûnal product was characterized by Fourier transform infrared spectroscopy (FT-IR), thermal gravimetric analysis (TGA), transmission electron microscopy (TEM), scanning electron microscopy (SEM), and UV-visible absorption and ûuorescence emission. The material was found to demonstrate selective interactions with Hg^{2+} ions. This interaction is most probably due to the presence of the ûuorophore moiety at the surface of nanomaterial. Fluorescence measurements revealed that the emission intensity of the Hg^{2+}-bound with the magnetic core-shell Fe$_3$O$_4$@SiO$_2$ NPs increases signiûcantly upon addition of various concentrations of Hg^{2+}, while in case of other mono, di, trivalent cations no changes or weak changes in the intensities were observed. The enhancement of ûuorescence is attributed to the strong covalent binding of Hg^{2+} ions with the binding constant value of 1.7×10^5/M. The sensor can be applied for analysis of mercury in environmental sample.

Key words: Mercury ion, Fluorescent probe, Nano-chemosensor, Functionalized magnetic core-shell Fe$_3$O$_4$@SiO$_2$ nanoparticles

INTRODUCTION

Since heavy metal ions can cause severe risks for human health and the environment, methods for the facile preparation of fluorescence receptors with high selectivity and sensitivity for heavy metal ions have received much attention. Among the known heavy metal ions, mercury is one of the most toxic heavy metals in the environment. Different forms of mercury can be accumulated in animals and plants. Mercury can damage central nerve by entering into human body from food cycle (Krämer 1998; Fabbrizzi and Poggi,

1995). As an environmental widely dispersed element, mercury can be destructive to natural metabolism, incretion and procreate of organism, leading to maladjustment in hormone secretion. Thus, it is important to develop a safe and effective procedure to detect mercury in environmental samples.

The most widely used methods for determination of mercury are cold vapour atomic absorption spectrometry (Zhang and Adeloju, 2008), cold vapour atomic fluorescence spectrometry (Cava-Montesinos *et al.,* 2004), X-ray fluorescence spectrometry (Aretaki

*Corresponding author E-mail: ganjali@khayam.ut.ac.ir

et al., 2006), inductively coupled plasma-mass spectrometry (Nixon *et al.,* 1999), potentiometric ion selective electrodes (Gupta *et al.,* 2005; 2007) and (voltammetry (Bonfil *et al.,* 2000). With regard to sensitivity and accuracy, these methods are efficient tools for mercury determination, but they are time-consuming, expensive and require sophisticated equipment (Mckenzie and Smythe, 1998). Thus, much interest has attended to the development of fluorescent sensors that offer distinct advantages in terms of sensitivity, selectivity, response time and remote sensing (Lakowicz, 1999; Desvergne and Czarnic, 1997; Ganjali *et al.,* 2009a; b; Hosseini *et al.,* 2011a; b).

Magnetic core-shell $Fe3O4@SiO_2$ nanoparticles, as special immobilizing carrier of biomolecules, have attracted great interest in current researches because they are biocompatible, easily renewable, and are stable against degradation (Fang and Zhang, 2009; Gao *et al.,* 2009). The inner iron-oxide core with outer shell of silica stabilizes the nanoparticles in the solution and also provides sites for surface modification with various biomedical ligands in biomedical applications (See *et al.,* 2005).

Usually, an inert silica coating on the surface of magnetite nanoparticles prevents their aggregation in the solution, improves their chemical stability, and provides better protection against toxicity (Lesnikovich *et al.,* 1990). In particular, the magnetic nanoparticles can also provide efficient binding to the guest molecules due to their high surface-to-volume ratio (Lee *et al.,* 2009).

Searching for new type of fluorescent carriers with excellent analytical characteristics is of considerable interest. The Schiff bases derivatives, for instance, can be a good selectophores for transition metal cations (Gupta *et al.,* 2006). We investigated them in our laboratory as a new type fluorophore for optical chemosensing (Hosseini *et al.,* 2010a; b). Coumarins belong to a category of important fluorescent chromogens (Wheelock, 1959). Many coumarin derivatives have been used extensively as fluorescent brightening agents and narrow-band pulsed dye lasers (Duarte and Piper, 1980; Kwen *at al.,* 1989). To date, these categories of compounds have rarely been used as fluorescent carriers for optical chemo sensing.

With this in mind, we synthesized a novel organic–inorganic hybrid fluorescent sensor which fabricated by covalently anchoring 3-(benzo[*d*]thiazol-2-yl)-7-hydroxy-2*H*-chromen-2-one moiety on the surface of silicagel encapsulated maghemite nanoparticles (denoted as [BTC-$Fe_3O_4@SiO_2$]), as a fluorescent chromophore. Herein, we report the synthesis of a ''turn-on'' fluorescent chemosensor BTC-$Fe_3O_4@SiO_2$

with high selectivity and sensitivity to detect Hg^{2+} ion over other metal ions in trace amount. These particles have extensive potential for serving as a very useful tool for facilitating biotechnology applications.

MATERIALS & METHODS

All chemicals were of the reagent–grade from Fluka and Merck chemical companies (Germany). The nitrate and chloride salts of all cations used (all from Merck, Germany) were of the highest purity available and used without any further purification except for vacuum drying over P_2O_5. Tetraethyl orthosilicate (TEOS) and 3-chloropropyltrimethoxysilane (CPTMS) were purchased from Merck (Germany). All other reagents and solvents were of analytical grade and used as received.The 3-cyanocoumarin and 3-(benzo[*d*]thiazol-2-yl)-7-hydroxy-2*H*-chromen-2-one were synthesized using reported methods (Khoobi *et al.,* 2011a; b).

The ^1H and ^{13}C NMR spectra were recorded using a Bruker 500 spectrometer (Bruker, Rheinstatten, Germany), and chemical shifts are expressed as δ (ppm) related to tetramethylsilane (TMS) as internal standard. The IR spectra were taken using a Nicolet FT-IR Magna 550 spectrographs (KBr disks) (Nicolet, Madison, WI, USA) within a 4000–400. SEM analysis was performed on a Philips XL-30 field-emission scanning electron microscope operated at 16 kV while TEM was carried out on a Tecnai G2 F30 at 300 kV. The experiments were performed using a microwave oven (ETHOS 1600, Milestone) with a power of 600 W specially designed for an organic synthesis and modified with a condenser and mechanical stirrer. The TGA thermograms were obtained from a PL-Thermal science PL-STA 1500 instrument. The emission spectra were obtained on a Perkin-Elmer LS50 luminescence spectrometer. Fluorescence measurements were done in a 1 cm quartz cuvette containing a magnetic-stirred suspension of BTC-$Fe_3O_4@SiO_2$ (20 mg/L) in 3 mL of acetonitrile - water solution (20/80, v/v). This solution was titrated with standardized Hg^{2+} ion solution and the fluorescence intensity of the system was measured. The emission intensity was measured at an excitation wavelength of 360 nm. Spectral bandwidths of monochromators for excitation and emission were 5 nm.

Fe_3O_4 nanoparticles were synthesized via the co-precipitation of Fe^{2+} and Fe^{3+} ions (molar ratio 1:2) in alkali solution. $FeCl_3 \cdot 6H_2O$ (3.7 mmol) and $FeCl_2 \cdot 4H_2O$ (1.85 mmol) were dissolved in 30 mL deionized water and the resulting solution was dropped to a 25% NH_4OH solution (10 mL) with precisely constant drop rate under nitrogen gas and vigorous mechanical stirring (800 rpm) to obtain small and uniform particles. A black precipitate of Fe_3O_4 was continuously stirred

for 1 h at room temperature and then heated to 80 °C for 2 h. The desire Fe_3O_4 was collected by a permanent magnet, followed by washing three times with deionized water, EtOH and drying at 100 °C in vacuum for 24 h. Prior to coat the Fe_3O_4 with a layer of silica, a sample of Fe_3O_4 (1 g) obtained previously suspended thoroughly with ultrasonic bath in methanol (80 mL) for 1 h at 40°C. Then concentrated ammonia solution was added to the resulting mixture and stirred at 40°C for 30 min. Afterward, tetraethyl orthosilicate (TEOS, 1.0 mL) was introduced to the reaction vessel, and continuously stirred at 40°C for 24 h. The silica-coated magnetic nanoparticles were separated by a permanent magnet, followed by washing several times with EtOH, diethyl ether and drying at 60 °C in vacuum for 24 h. In the next step, a sample of silica coated magnetic nanoparticle (500 mg) which suspended in dry toluene containing 1 mL of 3-chloropropyltrimethoxysilane (CPTMS) was refluxed for 6 h and the solid ($Fe_3O_4@SiO_2$-Si-$(CH_2)_3$-Cl) was separated, washed with dry toluene and dried in vacuum for 24 h at room temperature. The solid (-Cl) was separated, washed several times with dry toluene, MeOH, acetone and drying at 60æ%C in vacuum for 24 h.

3-(benzo[*d*]thiazol-2-yl)-7-hydroxy-2*H*-chromen-2-one were prepared according to the literature (Hosseini *et al.*, 2010a). To a mixture of 3-cyanocoumarin **1** (1 mmol) and 2-aminothiophenol **2** (1.2 mmol) was added 3 ml AcOH as solvent and catalyst and the mixture was irradiated with microwaves at 300 W for 15 min. After completion of the reactions, the mixture was cooled and the precipitated solid was filtered out and washed with Et_2O and water. Further purification was carried out by crystallization from EtOH giving red solid.

300 mg of as-synthesized $Fe_3O_4@SiO_2$-Si-$(CH_2)_3$-Cl was suspended thoroughly with ultrasonic bath in dry acetonitrile (5 mL) for 1 h at room temperature. Then 3-(benzo[*d*]thiazol-2-yl)-7-hydroxy-2*H*-chromen-2-one **3** (1 mmol) were dissolved in 5 mL acetonitrile following by addition of 1 mL of triethylamine and the resulting solution was added to the suspension of magnetic particle under nitrogen gas with vigorous stirring. The resulting solution was continuously stirred for 48 h under reflux condition. The product was separated by external magnet, washed with ethanol, acetone and dried under vacuum for 24 h at 50æ%C to give the solid surface bonded to the 3-(benzo[*d*]thiazol-2-yl)-2*H*-chromen-2-one motif.

RESULTS & DISCUSSION

BTC-$Fe_3O_4@SiO_2$ was synthesized according to the procedure shown in Scheme 1. To confirm the surface modification of the BTC-$Fe_3O_4@SiO_2$, NMR technique could not be used because of the superparamagnetic nature of catalyst's core. Hence, core-shell magnetic nanocrystallitie were characterized by FTIR (Fig. 1), SEM, TEM and TGA (Fig. 2-4). The infrared (IR) spectra of BTC–$Fe_3O_4@SiO_2$ are shown in Fig. 1. The successful conjugation of BTC onto the surface of the $Fe_3O_4@SiO_2$ nanoparticles can be confirmed by infrared spectra. The bands at 3300-3500/cm and 1000-1300/cm of the both samples are ascribed to the O-H and Si-O stretching vibration on silanol (Peng *et al.*, 2011). BTC–$Fe_3O_4@SiO_2$ exhibited a v_{lacton}(C=O) vibration at 1723/cm and it is attributed to the coumarin ring. Quantitative determination of the functional group contents of the surface-bonded [BTC–$Fe_3O_4@SiO_2$] nanocrystallites was performed using thermo-gravimetric analysis (TGA) and a loading of 0.35 ± 0.01 mmol/g was obtained. TGA analysis of the immobilized BTC moiety was performed and showed a first peak due to desorption of the water (centered at 95°C). This is followed by a second peak around 300 until 600 °C, corresponding to the loss of the organic spacer group (Fig. 2). The SEM and TEM showed that the average size of synthesized encapsulated nanoparticles is less than 30 nm and they present as uniform particles SEM (Fig. 3) and (Fig. 4).

In order to evaluate whether BTC–$Fe_3O_4@SiO_2$ could be used as a selective fluorescent chemosensor for Hg^{2+} ion, we recorded the emission fluorescence spectra variations that occur upon addition of increasing amount of the cations (1×10^{-4} M) to an acetonitrile -water (20/80, v/v) solution of the ligand (0.02 g/L) at 25.0 ± 0.1°C. The resulting fluorescence intensity for the case of cations is shown in Fig. 5. As it is obvious from Fig. 5, the intensity of emission band at 460 nm enhanced with addition of Hg^{2+} ions. Other metal ions revealed no such addition in the emission band under the same conditions except Pb^{2+} ion that indicate a little quenching.

The UV-Vis absorption spectra of the mesoporous material BTC–$Fe_3O_4@SiO_2$ showed three absorption maxima at approximately 219, 252 nm and 380 nm. The mode of coordination of BTC–$Fe_3O_4@SiO_2$ with Hg^{2+} has been investigated by spectrophotometric titration at 298 K (0.2 g/L) suspended in acetonitrile -water (20/80, v/v) solution. Figure 6 shows typical UV-Vis titration curves of BTC–$Fe_3O_4@SiO_2$ with different concentrations of Hg^{2+} added. It is apparent from Figure 6 that the absorption intensity of BTC–$Fe_3O_4@SiO_2$ at 380 nm and 252 gradually decreases as the concentration of Hg^{2+} decreases stepwise. In addition, there were a well-defined isosbestic points at 239 nm, respectively. It indicates that a stable complex was present having a certain stoichiometric ratio between the receptor BTC–$Fe_3O_4@SiO_2$ and Hg^{2+} formed.
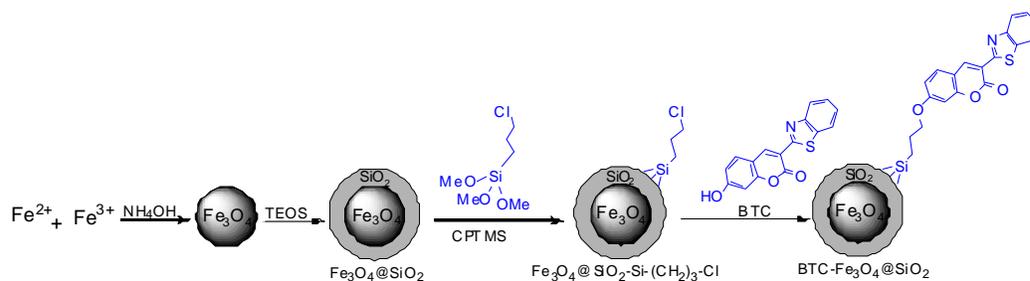
Scheme 1. Synthesis route of BTC–Fe$_3$O$_4$@SiO$_2$
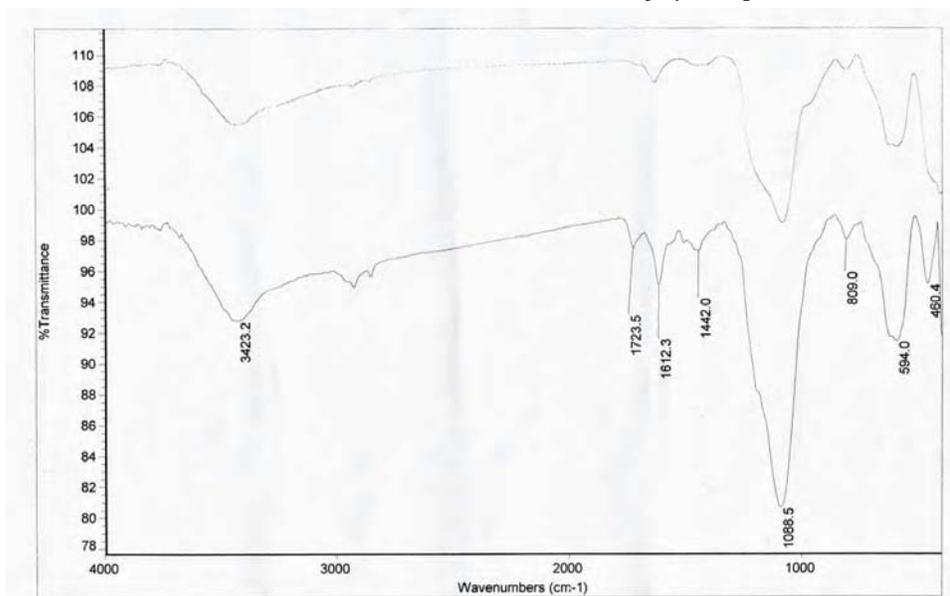
Fig. 1. IR spectra of BTC–Fe$_3$O$_4$@SiO$_2$ (a) the infrared (IR) spectra of BTC–Fe$_3$O$_4$@SiO$_2$ b) conjugation of BTC onto the surface of the Fe$_3$O$_4$@SiO$_2$ nanoparticles
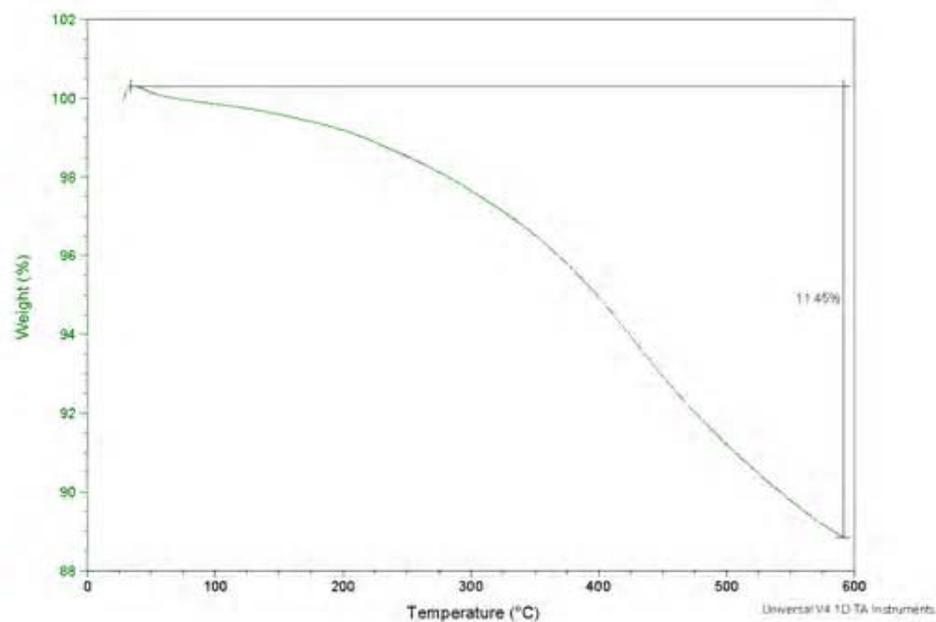
Fig. 2. TGA image of BTC–Fe$_3$O$_4$@SiO$_2$
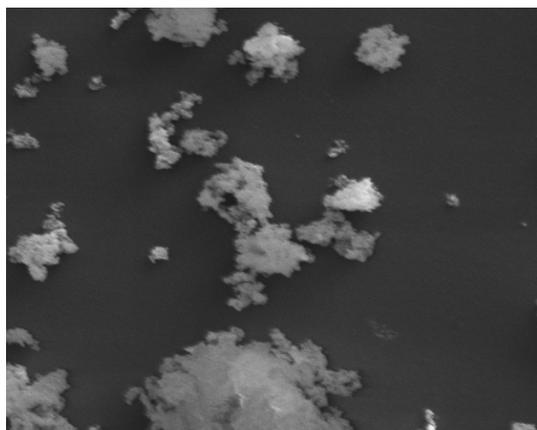
Fig. 3. SEM image of BTC–Fe₃O₄@SiO₂
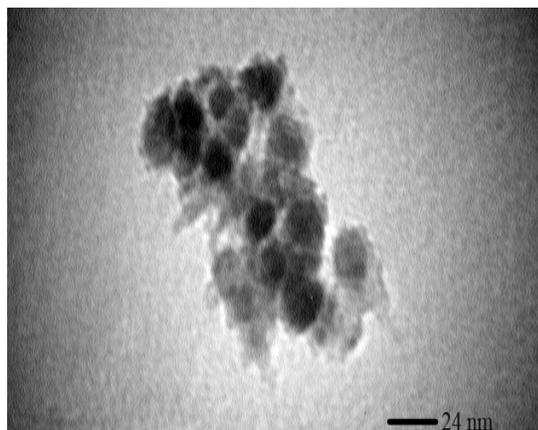
Fig. 4. TEM spectra of BTC–Fe$_3$O$_4$@SiO$_2$
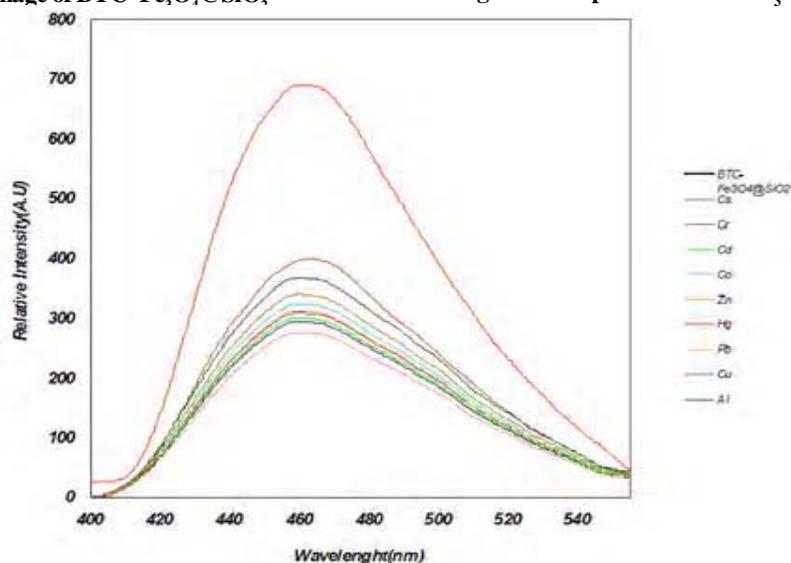
Fig. 5. Fluorescence emission spectra of BTC–Fe$_3$O$_4$@SiO$_2$ (3 ml 0.8mg/L) suspended in acetonitrile -water **(20/80, v/v) solution in the presence of different metal ions (1.0×10⁻⁴M). Excitation was performed at 360 nm.**
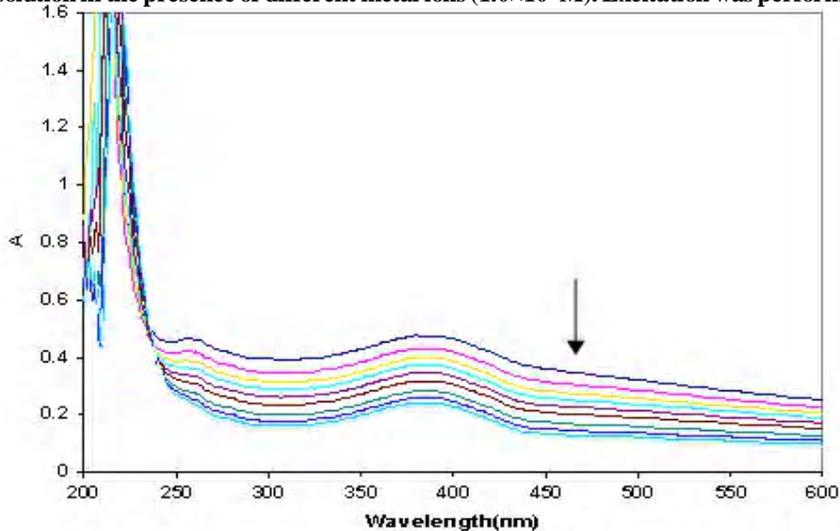
Fig. 6. UV-vis spectra change of BTC–Fe$_3$O$_4$@SiO$_2$ (3 ml 0.1 gr/L) upon addition of Hg²⁺ (1.0×10⁻³M) in acetonitrile **-water (20/80, v/v) solution**

All of the fluorescence titration experiments were performed in a suspended aqueous solution and the maximum excitation wavelength was selected at 360 nm. As illustrated in Fig. 7, BTC–Fe$_3$O$_4$@SiO$_2$ showed a typical emission band around 460 nm, which was considerably enhanced in the presence of Hg^{2+} ions. This phenomenon may occur a large CHEF (chelation-enhanced fluorescence) effect in the emission spectra, resulting from the blocking of the PET process (Valeur and Leray, 2000; Prasanna de silva *et al.,* 2000). When the concentration of Hg^{2+} ions was increased up to 2.0×10^{-6} M, more than 80% enhancing of the initial fluorescence of BTC–Fe$_3$O$_4$@SiO$_2$ was observed (Fig. 7). The detection limit of BTC–Fe$_3$O$_4$@SiO$_2$ as a fluorescent sensor for the analysis of Hg^{2+} was studied from the plot of the fluorescence intensity as a function of the concentration of added cations and it was found that BTC–Fe$_3$O$_4$@SiO$_2$ has a detection limit of 1.6×10^{-7} M for Hg^{2+} ions with linear range of 0.33-3.6 μM (Bühlmann *et al.,* 1997).

Here $\Delta F = F_x - F_0$ and $\Delta F_{max} = F\infty - F_0$, where F_0, F_x, and $F\infty$ are the emission intensities of BTC–Fe$_3$O$_4$@SiO$_2$ considered in the absence of Hg^{2+}, at an intermediate Hg^{2+} concentration and at a concentration of complete interaction, respectively, and where K is the binding constant and [C] the Hg^{2+} concentration. From the plot of $(F\infty - F_0)/(F_x - F_0)$ against $[Hg^{2+}]^{-1}$ (Fig. 8), the value of K extracted from the slope is 1.7×10^5/M.
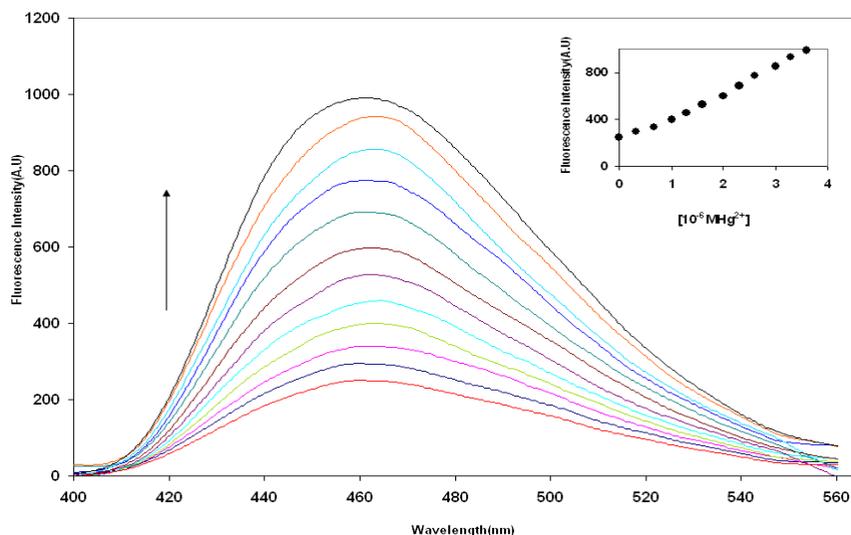
Fig. 7. Excitation(A) and Emission(B) spectra of the proposed chemosensor in the prescence of varying concentration of Hg^{2+} ions: (1) 0,(2) 3.3×10^{-7}M,(3) 6.3×10^{-7}M, (4) 1.0×10^{-6}M, (5) 1.3×10^{-6}M, (6) 1.6×10^{-6}M (7) 2.0×10^{-6}M, (8) 2.3×10^{-6}M, (9) 2.6×10^{-6}M, (10) 3.0×10^{-6}M, (11) 3.3×10^{-6}M, (12) 3.6×10^{-6}M, , λ_{ex}= 360nm.
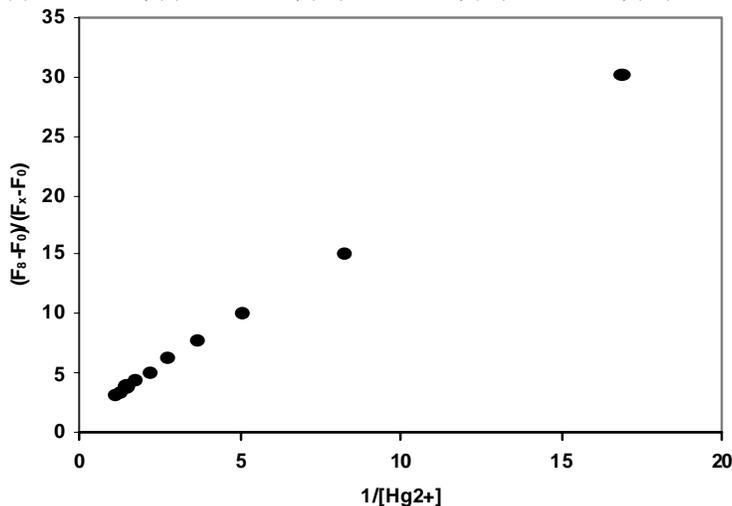
Fig. 8. Determination of the binding constant, K(±10%) of Hg^{2+} with BTC–Fe$_3$O$_4$@SiO$_2$

866

The selectivity behavior is obviously one of the most important characteristics of a chemosensor, which is the relative sensor response for the primary ion over other ions present in the solution. To examine the selectivity of the proposed nano-chemosensor, its affinity to other metal ions, including all mono, bivalent metal ions and trivalent ions were measured. The influence of interfering ions such as Na^+, Ca^{2+}, Cs^+, Sr^{2+}, Cu^{2+}, Zn^{2+}, Cd^{2+}, Hg^{2+}, Al^{3+}, Co^{2+}, Pb^{2+}, Cr^{3+}, La^{3+}, Ce^{3+} and Dy^{3+} on the fluorescence behavior of BTC–$Fe_3O_4@SiO_2$ (20 mg/L) was shown in Fig. 9. A fluorescence quenching was detected upon the addition of Cu^{2+}, however, a fluorescence enhancement was observed for BTC–$Fe_3O_4@SiO_2$ upon binding Hg^{2+} by comparison with that only BTC–$Fe_3O_4@SiO_2$ in the solution. No obvious change in the fluorescence intensity was observed even when double equivalents of other metal ions were used.

The competition measurements were carried out by the subsequent addition of $5×10^{-4}$ M metal ions to the solution of BTC–$Fe_3O_4@SiO_2$ in aqueous solution. The ûuorescence spectra were recorded at 460 nm with the addition of these metal ions and the subsequent addition of ($5×10^{-4}$ M) Hg^{2+} ions to the above solutions. Fig. 9 illustrates that the enhancement in the ûuorescence intensity resulting from the addition of Hg^{2+} ion has not been signiûcantly inûuenced by the addition of mono, bivalent metal ions and trivalent lanthanide ions.

Consequently, the new hybrid material BTC–$Fe_3O_4@SiO_2$ can be used as a chemosensor for the detection of different concentrations of Hg^{2+} ion with high selectivity.

The high degree of mercury selectivity, exhibited by the proposed sensor, makes it potentially useful for monitoring of low level concentrations of mercury ion in different water samples. These samples were filtered two times through qualitative filter paper before use. The 10.0 ml of each water sample (tab and waste water samples) was taken and diluted with acetonitrile -water (20/80, v/v) solution in a 25.0 ml volumetric flask. Different amounts of mercury ions were added to water samples. The proposed method was used to determine the mercury content of the samples by using calibration method. The obtained results are summarized in Table 1. It was found that the accuracy of mercury detection in different solution samples is almost quantitative.

Also, complete magnetic separation of BTC–$Fe_3O_4@SiO_2$ was achieved in 30 s by placing a magnet near the vessels containing the water dispersion of the nano-particles (Fig. 10). The magnetic separation capability of BTC–$Fe_3O_4@SiO_2$ nanoparticles in this detection method can also offer a simple route to separate Hg^{2+} - BTC–$Fe_3O_4@SiO_2$ system from various environment.
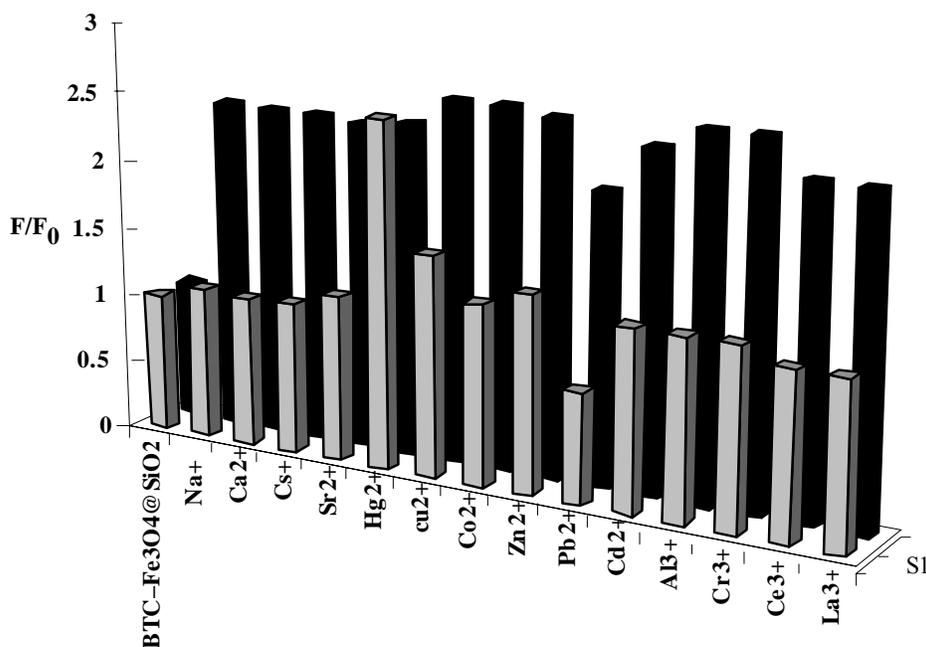
Fig. 9. (a) Gray bars represent relative fluorescence intensity of BTC–$Fe_3O_4@SiO_2$ (0.04 g/lit) in the presence of various cations (30 µmol/L) in the aqueous solution, $_{ex}$=360 nm, λ_{em}=460 nm,(b)Black bars represent relative fluorescence intensity of BTC–$Fe_3O_4@SiO_2$ (0.04gr/lit) containing 30 µmol/L cations and the background Hg^{2+} (30 µmol/L) (λ_{ex}: 360 nm)

Table 1. Determination of mercury ion in water samples and waste water with the present sensor

Sample	Added (mol/L)	Found [a] (mol/L)	Recovery (%)
Tap water	$4.1(\pm0.1) \times 10^{-6}$	$4.0 (\pm0.2) \times 10^{-6}$	97.5
River water	$2.2(\pm0.2) \times 10^{-6}$	$2.3(\pm 0.2) \times 10^{-6}$	104.5
Waste Water(Tehran)	$5.5(\pm0.2) \times 10^{-6}$	$5.4\pm(0.1) \times 10^{-6}$	98.2
Electroplating Factory)	$3.3(\pm0.3) \times 10^{-6}$	$3.2(\pm 0.2) \times 10^{-6}$	96.9

Fig.10. BTC–Fe_3O_4@SiO_2 responded to an external magnet

CONCLUSION

In summary, we have successfully designed and synthesized magnetic core-shell Fe_3O_4@SiO_2 nanoparticles functionalized by BTC which acts as a fluorescent chemosensor for Hg^{2+} ion solution. This work provides a platform to report magnetic nanoparticles modified by organic fluorescent chemosensor with high affinity, selectivity and sensitivity to detect metal ions.

ACKNOWLEDGEMENT

REFERENCES

Aretaki, I. N., Koulouridakis, P. and Kallithrakas-Kontos, N. (2006). Total reflection X-ray fluorescence mercury analysis after immobilization on quartz surfaces. Analytica Chimica Acta, **562 (2)**, 252-257.

Benesi, H. A. and Hildeb rand, J. H. (1949). A Spectrophotometric Investigation of the Interaction of Iodine with Aromatic Hydrocarbons. Journal of the American Chemical Society, **71 (8)**, 2703-2707.

Bonfil, Y., Brand, M. and Kirowa-Eisner, E. (2000). Trace determination of mercury by anodic stripping voltammetry at the rotating gold electrode. Analytica Chimica Acta, **424 (1)**, 65-76.

Bühlmann, P., Pretsch, E. and Bakker, E. (1997). Carrier-Based Ion-Selective Electrodes and Bulk Optodes. 1. General Characteristics. Chemical Reviews, **97 (8)**, 3083-3112.

Cava-Montesinos, P., Ródenas-Torralba, E., Morales-Rubio, A., Cervera, M.L. and Guardia, M. (2004). Cold vapour atomic fluorescence determination of mercury in milk by slurry sampling using multicommutation. Analytica Chimica Acta, **506 (2)**, 145-153.

Desvergne, J. P. and Czarnic, A. W. (1997). Chemosensors for ion and molecule recognition, Dordecht: Kluwer Academic Publishers.

Duarte, F. J. and Piper, J. A. (1980). A double-prism beam expander for pulsed dye lasers. Optics Communications, **35(1)**, 100-104.

Fabbrizzi, L. and Poggi, A. (1995). Sensors and switches from supramolecular chemistry. Chemical Society Reviews, **24(3)**, 197-202.

Fang, C. and Zhang, M. (2009). Multifunctional magnetic nanoparticles for medical imaging applications. Journal of Materials Chemistry, **19 (35)**, 6258-6266.

Ganjali, M.R., Hosseini, M., Hariri, M., Faridboda. F. and Norouzi. P. (2009a). Novel erbium (III)-selective fluorimetric bulk optode. Sensors and Actuators B, **142**, 90-96.

Ganjali, M.R., Veismohammadi, B., Hosseini, M. and Norouzi, P. (2009b). A new Tb^{3+}-selective fluorescent sensor based on 2-(5-(dimethylamino)naphthalen-1-ylsulfonyl)-N-henylhydrazinecarbothioamide. Spectrochimica Acta A, **74 (2)**, 575-578.

Gao, J., Gu, H. and Xu, B. (2009). Multifunctional Magnetic Nanoparticles: Design, Synthesis, and Biomedical Applications. Accounts of Chemical Research, **42 (8)**, 1097-1107.

Gupta, V. K., Chandra, S. and Lang, H. (2005). A highly selective mercury electrode based on a diamine donor ligand, Talanta, **66**, 575-580.

Gupta, V. K., Singh, A. K., Mehtab, S. and Gupta, B. (2006). A cobalt(II)-selective PVC membrane based on a Schiff base complex of N,N2 -bis(salicylidene)-3,4-diaminotoluene, Analytica Chimica Acta, **566**, 5-10.

Gupta, V.K., Singh, A.K., Al Khayat, M. and Gupta, B. (2007). Neutral carriers based polymeric membrane electrodes for selective determination of mercury (II), Analytica Chimica Acta **590**, 81-90.

Hosseini, M., Vaezi, Z., Ganjali, M. R., Faridbod, F., Dehghan Abkenar, S., Alizadeh, K. and Salavati-Niasari, M. (2010a). Fluorescence "turn-on" chemosensor for the selective detection of zinc ion based on Schiff-base derivative. Spectrochimica Acta A, **75 (3)**, 978-982.

Hosseini, M., Vaezi, Z., Ganjali, M. R., Faridbod, F., Dehghan Abkenar, S. and Salavati-Niasari, M. (2010b). Selective Recognition of Mercury in Waste Water Based on Fluorescence Enhancement Chemosensor. Sensor Letter, **8 (6)**, 807-812.

Hosseini, M., Vaezi, Z., Ganjali, M. R., Faridbod, F. and Dehghan Abkenar, S. (2011a). Fluorescence "Turn-On" chemosensor for the selective detection of beryllium. Spectrochimica Acta A, **83 (1)**, 161-164.

Hosseini, M., Ganjali, M. R., Tavakoli, M., Norouzi, P., Faridbod, F., Goldooz, H., and Badiei, A. R. (2011b). Pyrophosphate Selective Rcognition in Aqueous Solution Based on Fluorescence Enhancement of a New Aluminium Complex. Journal of Fluorescence, **21 (4)**, 1509-1513.

Khoobi, M., Emami, S., Dehghan, G., Foroumadi, A., Ramazani, A. and Shafiee, A. (2011a). Synthesis and Free Radical Scavenging Activity of Coumarin Derivatives Containing a 2-Methylbenzothiazoline Motif. Archiv der Pharmazie, **344(9)**, 588-594.

Khoobi, M., Ramazani, A., Foroumadi, A., Hamadi, H., Hojjati, Z. and Shafiee, A. (2011b). Efficient Microwave-Assisted Synthesis of 3-Benzothiazolo and 3-Benzothiazolino Coumarin Derivatives Catalyzed by Heteropoly Acids. Journal of the Iranian Chemical Society, **8 (4)**, 1036-1042.

Krämer, R. (1998). Fluoreszenz-Chemosensoren für Cu^{2+}-Ionen: schnell, selektiv und hochempfindlich, Angewandte Chemie, **110 (6)**, 804-806.

Kwen, J. W., Jacll, L., Hee, L. M. and Chui, C. T. (1989). Power enhancement of energy transfer rhodamine 6G dye laser by dye mixing method. Sae. Mulli, **29 (6)**, 719-723.

Lakowicz, J. R. (1999). Principles of fluorescence spectroscopy. New York, Kluwer academic/Plenum Publishers.

Lee, H. Y., Bae, D. R., Park, J. C., Song, H., Han, W. S. and Jung, J. H. (2009). A Selective Fluoroionophore Based on BODIPY-functionalized Magnetic Silica Nanoparticles: Removal of Pb^{2+} from Human Blood. Angewandte Chemie International Edition, **48 (7)**, 1239-1243.

Lesnikovich, A. I., Shunkevich, T. M., Naumenko, V. N., Vorobyova, S. A. and Baykov, M. V. (1990). Dispersity of magnetite in magnetic liquids and the interaction with a surfactant. Journal of Magnetism and Magnetic Materials, **85(1-3)**, 14-16.

Mallick, A. and Chattopadhyay, N. (2005). Photophysics in Motionally constrained Bioenvironment: Interactions of Norharmane with Bovine Serum Albumin. Photochemistry and Photobiology, **81 (2)**, 419-424.

Mckenzie, H. A. and Smythe, L. E. (1998). Quantitative trace analysis of biological materials. New York, Elsevier.

Nixon, D. E., Burritt, M. F. and Moyer, T. P. (1999). The determination of mercury in whole blood and urine by inductively coupled plasma mass spectrometry. Spectrochimica Acta B, **54 (8)**, 1141-1153.

Peng, X., Wang, Y., Tang, X. and Liu, W. (2011). Functionalized magnetic core–shell Fe3O4@SiO2 nanoparticles as selectivity-enhanced chemosensor for Hg(II). Dyes and Pigments, **91**, 26-32.

Prasanna de silva, A., Fox, D. B., Huxley, A. J. M. and Moody, T. S. (2000). Combining luminescence, coordination and electron transfer for signalling purposes. Coordination Chemistry Reviews, **205 (1)**, 41-57.

See, K. H., Mullins, M. E., Mills, O. P., and Heiden, P. A. (2005). A reactive core–shell nanoparticle approach to prepare hybrid nanocomposites: effects of processing variables. Nanotechnology, **16(9)**, 1950-1959.

Valeur, B. and Leray, I. (2000). Design principles of fluorescent molecular sensors for cation recognition. Coordination Chemistry Reviews, **205**, 3-40.

Wheelock, C. E. (1959). The Fluorescence of Some Coumarins. Journal of the American Chemical Society, **81 (6)**, 1348-1352.

Zhang, Y. and Adeloju, S. B. (2008). A novel sequential injection-Cold vapour atomic absorption spectrometric system for rapid and reliable determination of mercury. Talanta, **74 (4)**, 951-957.